Volume 2, Number 1: 11-15, April 2004

International Journal of
Vascular Biomedical Engineering

Fluid Dynamic Efficiency of an Anatomically Correct Total Cavopulmonary Connection: Flow Visualizations and Computational Fluid Dynamic Studies

S H Yun, S Y Kim and Y H Kim[¶]

Biomechanics Laboratory, Department of Biomedical Engineering,
Research Institute of Medical Engineering,
Research Institute for Medical Instrumentation and Rehabilitation Engineering, Yonsei University

Abstract

Both flow visualizations and computational fluid dynamics were performed to determine hemodynamics in a total cavopulmonary connection (TCPC) model for surgically correcting congenital heart defects. From magnetic resonance images, an anatomically correct glass model was fabricated to visualize steady flow. The total flow rates were 4, 6 and 8L/min and flow rates from SVC and IVC were 40:60. The flow split ratio between LPA and RPA was varied by 70:30, 60:40 and 50:50. A pressure-based finite-volume software was used to solve steady flow dynamics in TCPC models. Results showed that superior vena cava(SVC) and inferior vena cava(IVC) flow merged directly to the intra-atrial conduit, creating two large vortices. Significant swirl motions were observed in the intra-atrial conduit and pulmonary arteries. Flow collision or swirling flow resulted in energy loss in TCPC models. In addition, a large intra-atrial channel or a sharp bend in TCPC geometries could influence on energy losses. Energy conservation was efficient when flow rates in pulmonary branches were balanced. In order to increase energy efficiency in Fontan operations, it is necessary to remove a flow collision in the intra-atrial channel and a sharp bend in the pulmonary bifurcation.

Key words: Congenital Heart Defect, Total Cavopulmonary Connection, Flow Visualization, Computational Fluid Dynamics, Fluid Dynamic Efficiency, Flow Collision, Swirling Fow

Introduction

Approximately, seven out of thousand newborn babies in Korea has congenital heart defects such as tricuspid atresia or univentricular heart[1], many of which interrupt or severely impair the flow of unoxygenated blood to the lungs. Fontan operations, by-passing the right ventricle, are performed for those congenital heart defects[2-4]. Up to now, so many Fontan surgical options have been reported, but can be classified in two major patterns: atriopulmonary and cavopulmonary connections. In the atriopulmonary connection (APC), the right atrium (RA) is connected to the pulmonary artery either by a graft or by direct anastomosis. The total cavopulmonary connection (TCPC) is a direct connection between vena cava and pulmonary arteries through an intra- or an extra-atrial conduit. Kim et al.[5] measured pressure drops and velocity fields in both APC and TCPC using pressure transducers and laser Doppler anemometer. De Laval et al.[3] performed flow visualization studies on transparent models of APC and TCPC. Their study described that flow separation and disturbances tended to occur downstream of the cavities, junctions, corners and stenoses. In vivo studies supported that as for energy conservation TCPC is more efficient than APC[6,7].

Energy conservation in TCPC procedure is very important, since there is a single functional ventricle to pump blood to both systemic and pulmonary circulations. Many researchers reported the effect of

¶ 234 Maeji, Heungup, Wonju, Kangwon, 220-710, Korea
Email: yhkim@dragon.yonsei.ac.kr

TCPC geometries on total energy and pressure losses. Ensley et al.[8] investigated the effects of curvature or flaring in TCPC models on the efficiency of the geometry and showed that collision of caval flow near the connection resulted in high dissipative energy losses and that the offset between the caval inlets reduced those losses. Sharma et al.[9] performed computational fluid dynamic (CFD) studies and reported a decrease in dissipated power with an increase of at least 1.0cm in caval offset. Ryu et al.[10] performed both in vitro experiments and CFD studies to find an optimal Fontan geometry to reduce fluid dynamic energy loss.

The purpose of the present study was to determine hemodynamic efficiency in an anatomically correct TCPC model using flow visualizations and CFD studies.

Materials and Methods

TCPC model

The TCPC model for the present study was based on magnetic resonance images of an eight-year old Fontan patient of pulmonary and tricuspid atresia. The MR images were obtained using a Philips Medical Systems ACS 1.5 Tesla scanner. A set of contiguous-transverse, cardiac gated, gradient-echo images were acquired from end systole to 100msec before the next R-wave as estimated from the patient's ECG tracing. The slice thickness for the images was 5.0mm and the slices overlapped by 1.0 mm. The repetition time was 18.0 msec, echo time (TE) 6.2msec, the flip angle 60 deg and the first-order gradient moment nulling (velocity compensation) was employed. Forty transverse slices were obtained to cover the entire Fontan geometry. The MR images were then transferred to the computer for image segmentation and 3-D reconstruction, which was performed by a pediatric radiologist. For computer reconstructions, portions of the segmented images to be excluded in the study, such as the left ventricle, aorta, etc. were eliminated from the images using a "lasso and cut" method. This left reconstructions of only those vessels which were important in Fontan connections. Using measurements taken from these computer reconstructions, Pyrex glass TCPC models were made for flow visualization studies, as shown in Figure 1. The model consisted of SVC, IVC, a part of RA, an intra-atrial conduit, the left pulmonary artery (LPA), and the right pulmonary artery (RPA).

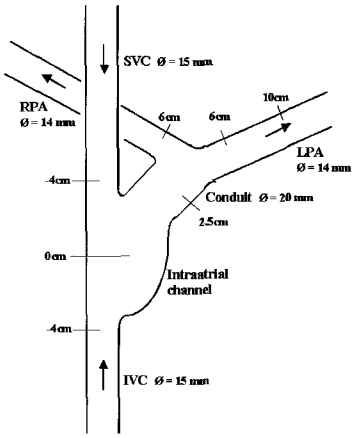

Figure 1 The TCPC model for the present study

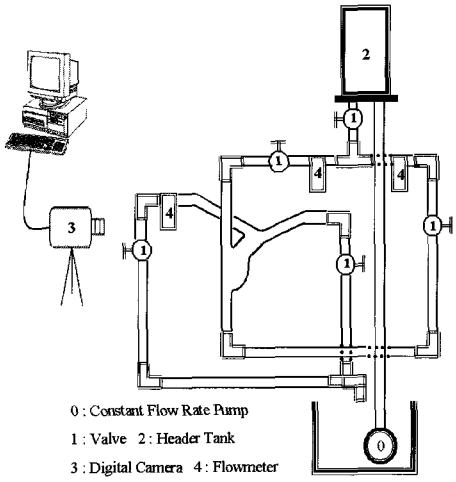

Figure 2 The schematic of the flow visualization set-up for steady flow

Flow visualizations

The schematic of the flow visualization set-up for steady flow is shown in Figure 2. Neutrally buoyant spherical Amberlite particles of 150μm diameter were added to the 40% glycerol solution. The TCPC model was illuminated with two 100W white lights to visualize flow patterns, and the particle streamlines were captured with a Panasonic NV-DJ100 digital video camera. Using a He-Ne laser, a sheet of light was created along the centreline of the model. The total flow rates were 4, 6 and 8 L/min, and flow rates of SVC and IVC were 40% and 60% respectively. The flow split ratio between LPA and RPA was varied by 70:30, 60:40 and 50:50.

Computational fluid dynamics

In vitro scaled model was scanned by a three-dimensional laser scanning system (Conveyor DS-2016, LaserDesign, U.S.A.) with a scan width of 5mm, and the

surface modelling was done using CFD pre-processing software, CFD-GEOM(CFDRC, U.S.A.). For the computational efficiency, a body-fitted grid was densely distributed at the intra-atrial channel and pulmonary bifurcation. Reynolds numbers based on inlet ranged from 581 to 1718 as in vitro experiments. Fluid was assumed to be Newtonian and incompressible. Assumptions of steady flow and rigid wall with no slip condition were also made. The density and the viscosity of the fluid were given by 1,090kg/m^3 and 0.036poise respectively. Inlet and outlet conditions were matched as those in flow visualization studies.

Governing equations to solve steady flow of incompressible and viscous fluid are as follows:

$$\frac{\partial u_i}{\partial x_i} = 0 \qquad (1)$$

$$\frac{\partial u_j u_i}{\partial x_j} = -\frac{1}{\rho}\frac{\partial p}{\partial x_i} + \frac{\mu}{\rho}\frac{\partial^2 u_i}{\partial x_j^2} \qquad (2)$$

where u is the fluid velocity, p is the pressure, and ρ is the density. Equation (1) is the continuity equation, and (2) is the momentum equation. A pressure-based finite-volume software, CFD-ACE, was used to solve governing equations in TCPC models.

Energy losses along typical streamlines in TCPC geometries were calculated. Energy loss per unit area calculated as in Equation (3).

$$e_n = \int_n p du_i - \int_{n+1} p du_i \qquad (3)$$

Results

Figures 3 and 4, obtained from flow visualizations and computational studies respectively at 6L/min, represent flow patterns in the intra-atrial conduit with different flow split ratios in pulmonary arteries. There were in good agreements between flow visualization pictures and corresponding CFD results. The collision of two opposite flow from SVC and IVC shifted toward SVC due to the larger amount of flow from IVC. In addition, two large vortices were found near the posterior-inferior and the posterior-superior walls in the intra-atrial channel. The former vortex is due to the geometry of the posterior-inferior wall in the intra-atrial channel, and the later is due to the collision of SVC and IVC flows.

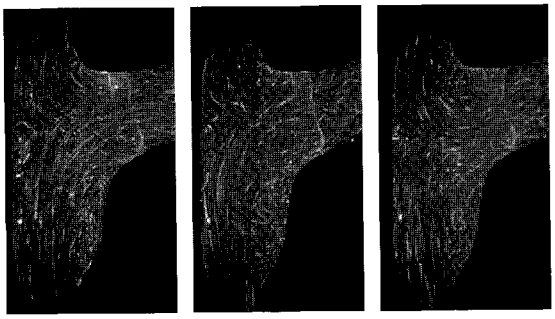

(a) LPA:RPA=70:30 (b) LPA:RPA=60:40 (c)LPA:RPA=50:50

Figure 3 Flow visualization pictures in the intra-atrial channel at 6 L/min.

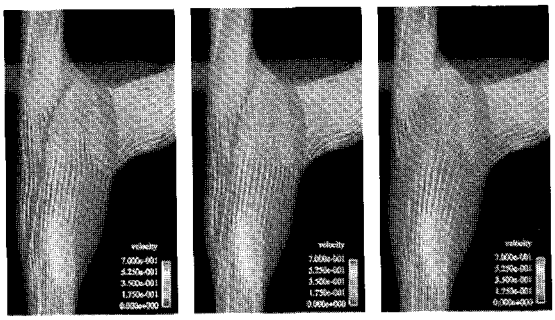

(a) LPA:RPA=70:30 (b) LPA:RPA=60:40 (c)LPA:RPA=50:50

Figure 4. Flow patterns from CFD study in the intra-atrial channel at 6 L/min

Mixed flow in the conduit was divided into LPA and RPA. Figure 5 shows flow visualization pictures and CFD results near the pulmonary bifurcation at 6 L/min at different flow split ratio at pulmonary branches. Flow visualizations and CFD results are in good agreement each other. Flow from the conduit stroke the posterior wall of the pulmonary bifurcation, resulting significant swirling motions in both pulmonary branches. This swirling motion was more significant in RPA due to the sharp bend between the conduit and RPA. Increased flow rates in RPA resulted in greater swirl motions, as shown in Figure 5(a) and (c).

Figure 6 shows calculated pressures at various locations along the centreline at 6L/min for different flow split ratios in pulmonary arteries. It is noted that a large pressure drop occurred between SVC and the conduit (about 100 Pa). On the other hand, there was a little pressure drop between IVC and the conduit (about 150 Pa). This is the reason why flow from SVC is smaller than that from IVC. RPA has larger pressure drops than LPA, which might be due to the sharp bend between the conduit and RPA. Smallest

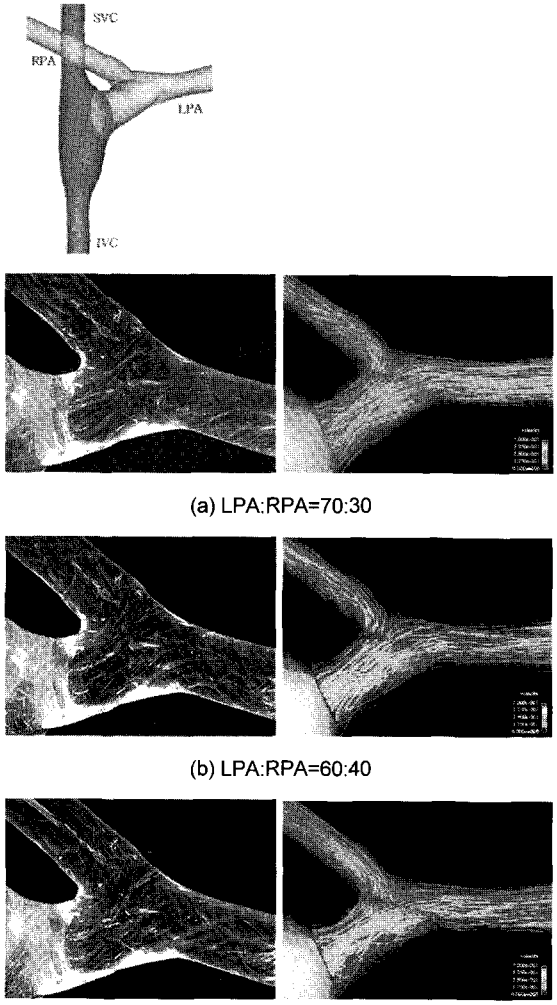

(a) LPA:RPA=70:30

(b) LPA:RPA=60:40

(c) LPA:RPA=50:50

Figure 5 Flow visualization pictures and CFD results near the pulmonary bifurcation at 6 L/min

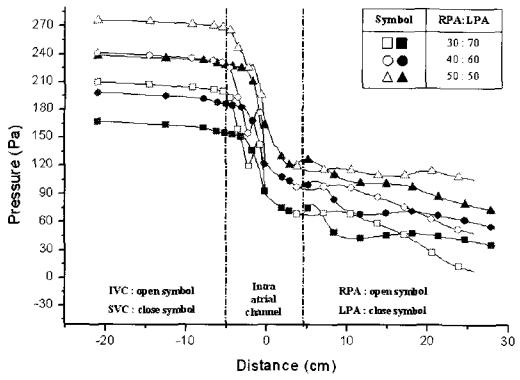

Figure 6 Calculated pressures in the TCPC model at 6 L/min for different flow split ratios in pulmonary arteries

pressure drops were observed when flow rates of LPA and RPA were balanced.

Figure 7 shows the accumulated energy loss for eight typical flow patterns from SVC and IVC when the flow split ratio of LPA and RPA is 30:70. Streamlines 3, 5 and 8 showed significantly large energy losses due to the flow collision and flow circulation in the intra-atrial channel. However, streamlines 2 and 7 had relatively small energy losses, showing smooth flow trajectories.

Figure 8 shows the accumulated energy loss for eight typical flow patterns from SVC and IVC with balanced flow rates at LPA and RPA. As in the figure, streamlines 1, 3 and 5 had significantly large energy losses due to the flow collision and the flow circulation in the intra-atrial channel. However, streamlines 6 and 7 showed relatively small energy losses.

Discussion and Conclusion

Since a single functional ventricle plays a role in both systemic and pulmonary circulations together, the energy efficiency in TCPC options is very important. We found that flow in the intra-atrial channel was very unstable due to the flow collision and circulating flow. This was more significant with higher flow rates. The TCPC model in this study is characterized by a sharp between the conduit and RPA. A sharp bend between the conduit and RPA made large vortices in the RPA. Previous studies[5,6,8,9] also reported that a sharp bend in Fontan operations should be removed in order to reserve energy efficiency.

Most of energy losses occurred at the intra-atrial channel and pulmonary bifurcation. Since swirling motions in Fontan connections result in energy loss, the present TCPC geometry might not be the most efficient Fontan model. Merged flow increases energy losses in Fontan connections[5,8-10]. In order to correct this flow dynamic inefficiency, it is necessary to remove a flow collision and a sharp bend in the pulmonary bifurcation. It was noted that the location of the flow division in pulmonary branches moved toward LPA with an increase of flow rate in RPA. Regions of flow separation or swirl motion might be susceptible for the occurrence of hemolysis and thrombosis in Fontan geometries[7].

Even though in reality flow in pulmonary arteries is pulsatile, steady flow was assumed in this study. However, pressure in the pulmonary circulation is relatively small compared to the systemic circulation, and the breathing effect also masks pulsatile flow effect[5,6,8-10]. Curt et al.[11]

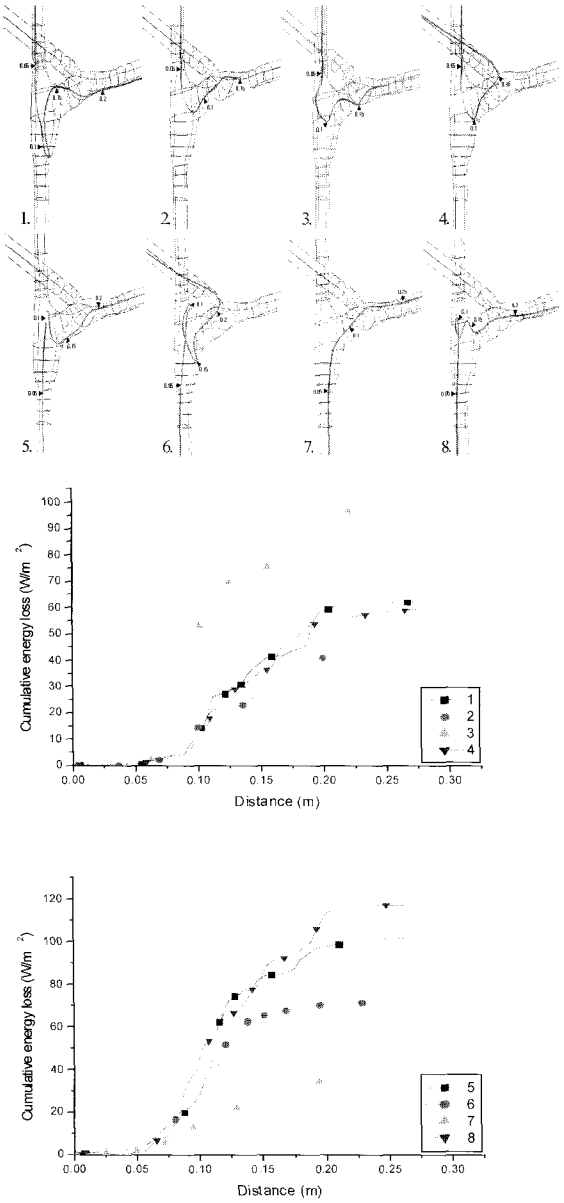

Figure 7 Accumulated Energy loss at 6L/min with flow split ratio of 70:30 at LPA and RPA

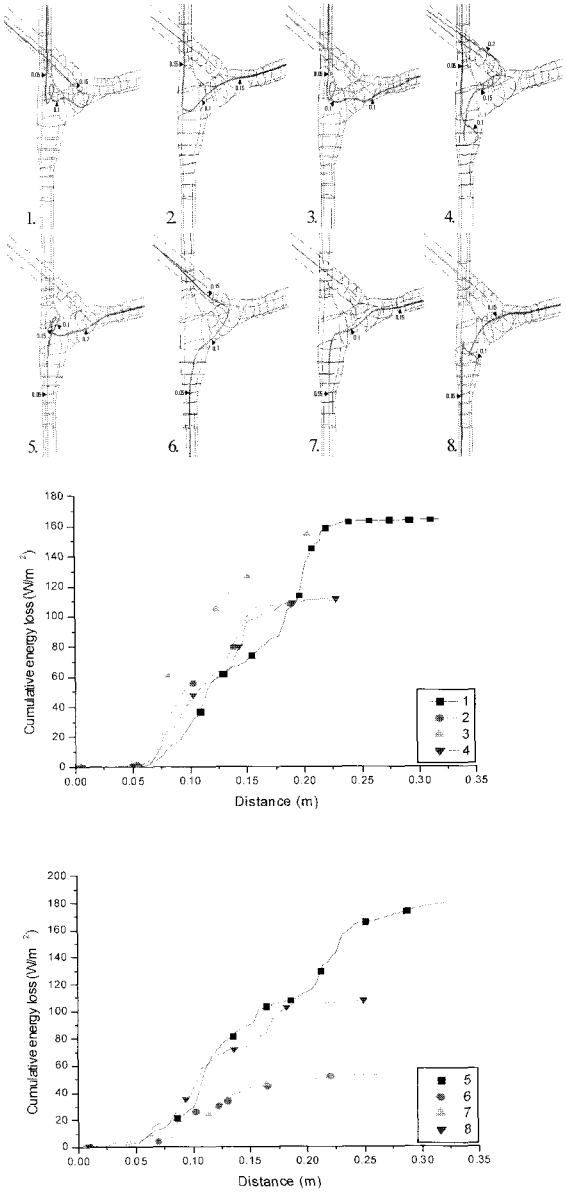

Figure 8 Accumulated Energy loss at 6L/min with flow split ratio of 50:50 at LPA and RPA

performed experiments on both steady and pulsatile flows in four different TCPC designs, having different offsets between SVC and IVC. They reported that overall power loss was smaller in steady flow than that in pulsatile flow.

In this study, three different flow split ratios between LPA and RPA were considered as 70:30, 60:40, and 50:50. Among those models, the smallest energy loss was found when both pulmonary arteries have balanced flow rates. Sharma et al.[9] also reported that pulmonary flow should be balanced in order to prevent the patients from atelectasis, diaphragm paralysis and pleural effusion.

In summary, both flow visualizations and CFD studies were performed to determine fluid dynamic efficiency in an anatomically correct TCPC model for Fontan surgeries. Significant flow collision and swirl motions in the intra-atrial channel and pulmonary arteries were observed. Swirling motion was more significant in RPA due to the sharp bend with the conduit. Large pressure drops occurred in the conduit and RPA. Flow collision and swirling motion in the intra-atrial channel resulted in large energy losses. A

sharp bend or a flow collision should be removed in order to increase fluid dynamic efficiency in Fontan surgical options.

Acknowledgements

This work was partially supported by RRC program of MOST and KOSEF.

References

1. Hoffman J.I.E., Incidence, In Anderson R.H., Macartney F.J., Shinebourne E.A. and Tynan M. (eds), Pediatric Cardiology, London; Churchill Livingstone, 1987.
2. Fontan F and Baudet E., Surgical repair of tricuspid atresia, Thorax, 1971, 26; 240-248.
3. Kreuzer G., Galindez E., Bono H., de Palma C. and Laura J.P. An operation for the correction of tricuspid atresia, J Thorac Cardiovasc Surg, 1973;66:613-621.
4. Bjork V.D., Olin C.L., Bjarke B.B. and Thoren C.A. Right atrial-right ventricular anastomosis for correction of tricuspid atresia, J Thorac Cardiovasc Surg, 1979;77: 452-459.
5. Kim Y.H., Walker P.G., Fontaine A.A., Panchal S., Ensley A.E., Oshinski J., Sharma S., Ha B., Lucas C.L. and Yoganathan A.P., Hemodynamics of the Fontan connection: an in vitro study, J Biomech Eng, 1995;117: 423-428.
6. De Laval M.R., Kilner P., Gewillig M. and Bull C., Total cavopulmonary connection: a logical alternative to atriopulmonary connection for complex Fontan operations, J Thorac Cardiovasc Surg, 1988;96:682-695.
7. Low H.T., Chew Y.T. and Lee C.N., Flow studies on atriopulmonary and cavopulmonary connections of the Fontan operations for congenital heart defects, J Biomech Eng, 1993;15:303-307.
8. Ensley A.E., Lynch P., George P. and Chatzimavroudis, Toward designing the optimal total cavopulmonary connection: An in vitro study, Ann Thorac Surg, 1999;68:1384-1390.
9. Sharma S., Goudy S., Walker P., Panchal S., Ensley A., Kanter K., Tam V., Fyfe D. and Yoganathan A., In vitro flow experiments for determination of optimal geometry of total cavopulmonary connection for surgical repair of children with functional single ventricle, J Am Coll Cardiol, 1996;27:1264-1269.
10. Ryu K.S., Healy T.M., Ensley A.E., Sharma S., Lucas C. and Yoganathan A.P., Importance of accurate geometry in the study of the total cavopulmonary connection: Computational simulations and in vitro experiments, Ann Biomed Eng, 2001;29:844-853.
11. Curt G., De Groff and Robin S., Designing the optimal total cavopulmonary connection: Pulsatile versus steady flow experiments, Med Sci Monit, 2002;8:41-45.